POLITECNICO DI TORINO
Repository ISTITUZIONALE

Negativity of the excess noise in a quantum wire capacitively coupled to a gate

(Article begins on next page)

02 May 2024

Negativity of the excess noise in a quantum wire capacitively coupled to a gate

F. Dolcini,[1] B. Trauzettel,[2,3] I. Safi,[4] and H. Grabert[5]

[1]*Scuola Normale Superiore and NEST-INFM-CNR, 56126 Pisa, Italy*
[2]*Instituut-Lorentz, Universiteit Leiden, 2300 RA Leiden, The Netherlands*
[3]*Department of Physics and Astronomy, University of Basel, 4056 Basel, Switzerland*
[4]*Laboratoire de Physique des Solides, Université Paris-Sud, 91405 Orsay, France*
[5]*Physikalisches Institut, Albert-Ludwigs-Universität, 79104 Freiburg, Germany*

The electrical current noise of a quantum wire is expected to increase with increasing applied voltage. We show that this intuition can be wrong. Specifically, we consider a single-channel quantum wire with impurities and with a capacitive coupling to nearby metallic gates and find that its excess noise, defined as the change in the noise caused by the finite voltage, can be negative at zero temperature. This feature is present both for large ($c \gg c_q$) and small ($c \ll c_q$) capacitive coupling, where c is the geometrical and c_q the quantum capacitance of the wire. In particular, for $c \gg c_q$, negativity of the excess noise can occur at finite frequency when the transmission coefficients are energy dependent—i.e., in the presence of Fabry-Pérot resonances or band curvature. In the opposite regime $c \lesssim c_q$, a nontrivial voltage dependence of the noise arises even for energy-independent transmission coefficients: at zero frequency the noise decreases with voltage as a power law when $c < c_q/3$, while, at finite frequency, regions of negative excess noise are present due to Andreev-type resonances.

I. INTRODUCTION

In equilibrium, the fluctuations of an observable are directly connected to the relaxation of its average value through the fluctuation-dissipation theorem.[1] In contrast, out-of-equilibrium fluctuations contain in general more information than the mere average values. Electron transport is a typical example: When a conductor is driven out of equilibrium by applying a finite bias voltage V, the frequency spectrum[2]

$$S(x, \omega, V) = \int_{-\infty}^{\infty} dt\, e^{i\omega t} \langle \Delta j(x,t) \Delta j(x,0) \rangle \qquad (1)$$

of the electrical current fluctuations $\Delta j(x,t) = j(x,t) - \langle j(x,t) \rangle$ cannot be directly related to the ac conductivity $\sigma(x, \omega)$. Here $\langle \cdots \rangle$ denotes the quantum-statistical average over the stationary nonequilibrium density matrix of the system in presence of the applied voltage V.

The expression (1) is the unsymmetrized version of the customarily defined[3,4] current noise, the latter being easily obtained as $S_{\text{sym}}(x, \omega, V) = (1/2)[S(x, \omega, V) + S(x, -\omega, V)]$. Unsymmetrized noise has recently attracted attention in mesoscopic physics, in that it can be directly measured by on-chip detectors, as proposed in Refs. 2 and 5, and experimentally realized for the first time in Ref. 6. In this experiment the noise is related to the photon-assisted current generated in a superconductor-insulator-superconductor (SIS) Josephson junction detector.

Differently from the dc current, the noise is in principle a position-dependent quantity;[7] the coordinate x in Eq. (1) can be associated with the point of measurement typically in the leads. The estimate of the actual value of the distance δ_x between x and the lead-wire contact depends on the device, the geometry of contacts, and the type of detector and there-fore goes beyond the purposes of the present work. Here we rather emphasize that, while at zero frequency the noise becomes independent of the position, at finite frequency a dependence on x arises.[8] Since in this paper finite-frequency noise is discussed, we keep the dependence on x explicitly.

Nonequilibrium noise provides insight into the mechanisms underlying electron transport. In the shot noise limit the differences with respect to the equilibrium situation are most significant. In particular, at zero frequency and zero temperature the equilibrium noise vanishes, whereas the nonequilibrium noise is in general finite. For instance, in a ballistic conductor with impurities the shot noise originates from the statistical transmission or reflection of the discrete charge carriers at the scatterers. If the electron-electron interaction can be neglected, the scattering matrix formalism[7] is applicable. In this case the shot noise at zero temperature reads[9–11]

$$S(\omega = 0, V) = \frac{e^2}{2\pi\hbar} eV \sum_n T_n(1 - T_n), \qquad (2)$$

where T_n are the transmission coefficients of the eigenchannels of the conductor and $e > 0$ is the elementary charge. Note that, as mentioned above, the shot noise is independent of the position x appearing in Eq. (1). Comparing Eq. (2) with the expression

$$G = \frac{e^2}{2\pi\hbar} \sum_n T_n \qquad (3)$$

for the conductance, one can see explicitly that, in view of the $(1 - T_n)$ suppression factors, the out-of-equilibrium noise cannot be expressed in terms G.

In comparison with the formidable efforts made lately to predict[12–16] and measure[6,17–20] the frequency dependence of the noise, not so much interest has been devoted to the in-

vestigation of the *voltage* dependence of the noise. Intuitively, one would expect that the noise should increase with the voltage V; this intuition is confirmed by Eq. (2) describing the simple case of a system of noninteracting electrons when both the energy dependence of the transmission coefficients and the band curvature can be neglected.

This intuition is, however, wrong in general. For a single-channel wire, for instance, Lesovik and Loosen[21] have shown that in the particular case where the transmission coefficient is nonvanishing only in an energy window δE, the Fermi energy lies within this energy window, and the temperature is sufficiently high ($k_B T \gg \delta E$), the shot noise in the regime $eV \gg k_B T$ is smaller than the equilibrium noise. In the opposite limit of a multichannel clean wire it has been demonstrated[22] that, although the *current* noise is always increasing with V, the *voltage* noise may decrease with bias. These results, however, are concerned with either the high-temperature regime or the semiclassical limit (number of channels tending to infinity) of transport. Since most of the experimental interest in mesoscopic conductors lies instead in quantum effects, the open question is whether similar behavior can occur in the deep quantum regime—i.e., for a finite number of channels at low temperatures, where $\hbar \omega \gg k_B T$. This paper aims at investigating this problem. We consider here a single-channel quantum wire at zero temperature. For simplicity, we discuss the spinless case, although our analysis can be easily generalized to spinful electrons. We analyze the conditions under which the noise, both at zero and at finite frequency, can decrease with bias and investigate, in particular, whether the excess noise

$$S_{\text{EX}}(x, \omega, V) = S(x, \omega, V) - S(x, \omega, 0),\qquad(4)$$

characterizing the change of the noise due to the finite voltage with respect to the equilibrium case, can be negative. The total noise $S(x, \omega, V)$ is, of course, always positive, as follows from the Wiener-Khintchine theorem.[23] A negative excess noise simply means that driving the system out of equilibrium by applying a voltage V reduces the noise in certain frequency regions with respect to its equilibrium value.

The noise spectrum (1) can be directly related to the current spectral density

$$j(x, \omega) = \int_{-\infty}^{\infty} dt e^{i\omega t} j(x, t)\qquad(5)$$

through the relation

$$S(x, \omega, V) = \frac{1}{2\pi} \int_{-\infty}^{+\infty} d\omega' \langle \Delta j(x, \omega) \Delta j(x, \omega') \rangle,\qquad(6)$$

where $\Delta j(x, \omega) = j(x, \omega) - \langle j(x, \omega) \rangle$. As a consequence of the continuity equation the net flux of current flowing into the conductor equals the time rate of change of the charge in the conductor. Explicitly,
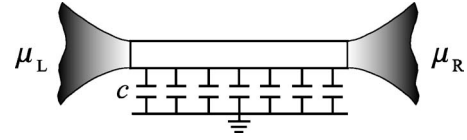

FIG. 1. Schematic of a quantum wire capacitively coupled to a nearby gate (with a capacitance per unit length c). The wire of finite length L is connected at $x = \pm L/2$ to reservoirs with electrochemical potentials μ_L and μ_R.

$$j\left(\frac{L}{2}; \omega\right) - j\left(-\frac{L}{2}; \omega\right) = \int_{-L/2}^{L/2} dx \,\text{div}\, j(x, \omega) = i\omega Q(\omega),$$

$$(7)$$

where $x = \pm L/2$ are the locations of the edges of the conductor of length L and

$$Q(\omega) = \int_{-\infty}^{\infty} dt e^{i\omega t} \int_{-L/2}^{L/2} dx \rho(x, t),\qquad(8)$$

with the charge density operator $\rho(x)$.

The wire is capacitively coupled to its electromagnetic environment consisting of other metallic conductors nearby. This gives rise to a *geometrical* capacitance C of the wire to the environment. The right-hand side of Eq. (7) can then be interpreted as the displacement current

$$j_d(\omega) = i\omega Q(\omega)\qquad(9)$$

through this capacitance C. Furthermore, the capacitive coupling induces a fluctuating shift $\Delta U(\omega) \sim Q(\omega)/C$ of the band-bottom of the wire which modifies the energy of the electrons, affecting in turn their scattering processes inside the conductor and therefore the current $j(x, \omega)$ itself. This feedback process makes the problem of determining finite frequency transport properties an essentially *interacting* problem.[7,24,25] In a dc-biased setup, the average current $I = \langle j(x, t) \rangle$ is independent of the position x and the time t, so that the *average* current spectral density is simply $\langle j(x, \omega) \rangle = 2\pi I \delta(\omega)$, and the displacement current has vanishing expectation value, as can be seen from Eqs. (7) and (9). For the noise, however, the full frequency dependence of the *fluctuations* of the current spectral density plays a role [see Eq. (6)], and the band-bottom shift induced by the displacement current fluctuations has to be taken into account.

In the present paper, we shall analyze the finite-frequency noise for the case of a ballistic single-channel quantum wire, capacitively coupled to a gate (see Fig. 1). For simplicity, we shall treat the capacitance C as uniformly distributed along the wire, $C = cL$, where c is the capacitance per unit length and L the length of the wire.[26] The Hamiltonian of the system thus reads

$$H = H_0 + H_{\text{imp}} + H_c.\qquad(10)$$

Here, H_0 describes the band kinetic energy of the electrons in the wire, H_{imp} the scattering with impurities if present, and

$$H_c = \frac{1}{2c} \int_{-L/2}^{L/2} \delta\rho^2(x) dx \qquad (11)$$

the capacitive coupling to the gate, where $\delta\rho(x) = \rho(x) - \rho_F$ is the deviation of the electron charge density $\rho(x)$ from the density ρ_F of an electroneutral wire. The capacitance c is a crucial quantity to determine the finite-frequency noise, for it relates the displacement currents to the band-bottom shift ΔU in the wire. In the regime $c \gg c_q$, where $c_q = e^2\nu$ is the quantum capacitance and ν is the density of states per unit length of the electron band described by H_0, it is evident that a finite displacement current yields a very small shift ΔU. The term (11) is then negligibly small with respect to H_0, and therefore the problem of determining the particle current decouples from the evaluation of the displacement current. For a finite capacitance, however, the two problems have to be solved simultaneously, and the band-bottom shift cannot be neglected. In this paper we investigate this problem. We are interested in the effects of the capacitive coupling between wire and metallic gate, and not in the effects arising from variations of the gate potential V_g; we therefore assume for definiteness that the gate is grounded $V_g = 0$.

The paper is organized as follows: In Sec. II, we analyze the case of a large geometrical capacitance (which corresponds to the noninteracting problem). In this case, we show that in a quantum wire with poorly transmitting contacts to the leads the excess noise can be negative at finite frequency. In Sec. III, we analyze the case of arbitrary geometrical capacitance. Thus, we discuss the fully interacting problem. In particular, we adopt a mapping between a capacitively coupled quantum wire and a Luttinger liquid model to predict that the excess noise can be negative even in presence of just a single impurity in the wire. Finally, we conclude in Sec. IV.

II. CASE OF LARGE CAPACITANCE

We first consider the case of large capacitance between wire and gate ($c \gg c_q$). Then the displacement current (which is always present to ensure charge conservation) does not induce a band-bottom shift in the wire. The term (11) can then be neglected and displacement currents play no role. We shall see that some interesting effects can still arise from band curvature or an energy dependence of the transmission coefficients which shall therefore be retained. For a Hamiltonian

$$H_0 = -\frac{\hbar^2}{2m} \int_{-\infty}^{+\infty} \Psi^\dagger(x) \partial_x^2 \Psi(x) dx, \qquad (12)$$

with the usual parabolic dispersion, the expression for the electronic current reads

$$j(x) = \frac{e\hbar}{2mi} \{\Psi^\dagger(x)\partial_x\Psi(x) - (\partial_x\Psi^\dagger(x))\Psi(x)\}, \qquad (13)$$

where $\Psi(x)$ is the electron field operator. However, when the band dispersion is linearized to investigate the low-energy limit or when a discrete lattice model is considered, expres-

sion (13) has to be consistently modified in order to preserve the continuity equation for the solutions. For a Hamiltonian with linearized spectrum

$$H_0 = -i\hbar v_F \int [:\Psi_\rightarrow^\dagger(x)\partial_x\Psi_\rightarrow(x): - :\Psi_\leftarrow^\dagger(x)\partial_x\Psi_\leftarrow(x):]dx, \qquad (14)$$

the expression for the current reads

$$j(x) = ev_F[:\Psi_\rightarrow^\dagger(x)\Psi_\rightarrow(x) - \Psi_\leftarrow^\dagger(x)\Psi_\leftarrow(x):]. \qquad (15)$$

Here, $\Psi_\rightarrow$ ($\Psi_\leftarrow$) is the electron field operator for a right (left) moving particle, and the symbol $::$ denotes normal ordering with respect to the Dirac sea.[27] Similarly, in a tight-binding lattice model

$$H_0 = -\tau \sum_i (c_i^\dagger c_{i+1} + c_{i+1}^\dagger c_i), \qquad (16)$$

one obtains

$$j(x) = -\frac{e\tau}{\hbar}(c_i^\dagger c_{i+1} - c_{i+1}^\dagger c_i), \qquad (17)$$

where τ is the hopping energy, c_i annihilates a fermion on lattice site i, and $x = ia_0$ (with a_0 the lattice spacing and i the lattice index).

All these different types of models can be treated within the scattering matrix formalism.[7] Here we follow the standard notation and denote by a_{XE} (b_{XE}) the operators of incoming (outgoing) states of energy E at the side $X = R, L$ of the scatterers; the outgoing states are expressed in terms of the incoming states through the S matrix:

$$\begin{pmatrix} b_{LE} \\ b_{RE} \end{pmatrix} = \mathsf{S}(E) \begin{pmatrix} a_{LE} \\ a_{RE} \end{pmatrix}, \quad \mathsf{S}(E) = \begin{pmatrix} r(E) & t'(E) \\ t(E) & r'(E) \end{pmatrix}. \qquad (18)$$

The electron operator Ψ in the left lead can be written as a superposition of a_{LE} and b_{LE} for all energies, weighted by the related eigenfunctions $\alpha_{LE}(x)$ and $\beta_{LE}(x)$ of incoming and outgoing states (typically plane waves). The cases of a linearized spectrum and of a lattice model can be treated in the same way. Substituting the above energy mode expansion into expressions (13) and (15), or (17), and using Eq. (18), the time evolution of the current operator at a point x located in the left lead reads[7]

$$j(x,t) = \frac{e}{2\pi\hbar} \sum_{X_1, X_2 = R, L} \int_{E_B}^{E_T} \int_{E_B}^{E_T} dEdE' e^{i(E-E')t/\hbar}$$
$$\times A_L^{X_1 X_2}(E, E'; x) a_{X_1 E}^\dagger a_{X_2 E'}. \qquad (19)$$

Here, E_B and E_T denote the bottom and top values of the energy band of the channel. The current matrix elements $A_L^{X_1 X_2}$ are defined as

$$A_L^{LL}(E, E'; x) = \frac{1}{e} \frac{\Omega}{\sqrt{v(E)v(E')}}$$
$$\times [j_L^{\alpha E; \alpha E'}(x) + j_L^{\beta E; \beta E'}(x) r^*(E) r(E')$$
$$+ j_L^{\alpha E; \beta E'}(x) r(E') + j_L^{\beta E; \alpha E'}(x) r^*(E)],$$

$$A_L^{RR}(E,E';x) = \frac{1}{e}\frac{\Omega}{\sqrt{v(E)v(E')}}j_L^{\beta E;\beta E'}(x)t'^*(E)t'(E'),$$

$$A_L^{LR}(E,E';x) = \frac{1}{e}\frac{\Omega}{\sqrt{v(E)v(E')}}[j_L^{\beta E;\beta E'}(x)r^*(E)t'(E')$$
$$+ j_L^{\alpha E;\beta E'}(x)t'(E')],$$

$$A_L^{RL}(E,E';x) = \frac{1}{e}\frac{\Omega}{\sqrt{v(E)v(E')}}[j_L^{\beta E;\beta E'}(x)t'^*(E)r(E')$$
$$+ j_L^{\beta E;\alpha E'}(x)t'^*(E)], \quad (20)$$

where Ω is the total length of the system, $v(E)=\hbar^{-1}\partial E/\partial k$ the band velocity, and $j_L^{\alpha E;\beta E'}(x)$ are the matrix elements of the appropriate current operator[28] in the basis of the eigenfunctions $\alpha_{LE}(x)$ and $\beta_{LE'}(x)$. For instance, for electrons with parabolic dispersion relation

$$j_L^{\gamma E;\gamma' E'}(x) = \frac{\hbar e}{2mi}[\gamma_{LE}^*(x)\partial_x\gamma'_{LE'}(x) - (\partial_x\gamma_{LE}^*(x))\gamma'_{LE'}(x)],$$
$$(21)$$

where $\gamma, \gamma' = \alpha, \beta$. Inserting then Eq. (19) into Eq. (1) and evaluating the averages with respect to the incoming electron operators a_{LE} and a_{RE}, the noise is easily determined. Notice that, differently from the customary assumptions of linear ized band and energy independent transmission coefficients which lead to Eq. (2), here Eq. (20) has been derived without any specific hypothesis about the band dispersion and the energy dependence of transmission coefficients.[29]

A. Voltage dependence of zero-frequency noise

To characterize the voltage dependence of the noise, we investigate the derivative $\partial S/\partial V$. In this section we consider the case $\omega = 0$; since we assume the temperature to be vanishing, no thermal noise sources are present and the noise at $\omega = 0$ can be identified with the shot noise. Denoting by μ_L and μ_R the electrochemical potentials of the left and right leads, we assume for definiteness $\mu_L - \mu_R = eV \geq 0$ and $E_B < \mu_L, \mu_R < E_T$. To be general, we consider an arbitrary way to apply the bias eV and set $\mu_{L/R} = E_F + \gamma_{L/R}eV$, where $\gamma_L \geq 0$ is an arbitrary coefficient and $\gamma_R = \gamma_L - 1$. Note that this is experimentally relevant in mesoscopic devices, where the bias is not always applied symmetrically.[30] We find that the voltage derivative of the noise at zero frequency and zero temperature is

$$\frac{\partial S}{\partial V}(\omega = 0, V) = \frac{e^3}{2\pi\hbar}[\gamma_L T(\mu_L)R(\mu_L) - \gamma_R T(\mu_R)R(\mu_R)],$$
$$(22)$$

where $T(E) = |t(E)|^2$ and $R(E) = 1 - T(E)$ are the (energy-dependent) transmission and reflection coefficients, respectively. As mentioned above, the shot noise is independent of the point of measurement x. The related expression for the differential conductance $G(V) = dI(V)/dV$ reads

$$G(V) = \frac{e^2}{2\pi\hbar}[\gamma_L T(\mu_L) - \gamma_R T(\mu_R)]. \quad (23)$$

Our results, Eqs. (22) and (23), are quite general, since they hold for any dispersion relation, for electrons in the continuum, for Bloch electrons, for lattice models, and for any number of scatterers. The only underlying hypothesis made is that electrons in the wire do not experience any band-bottom shift originating from the coupling to the gate ($c \gg c_q$). When the transmission coefficient is energy independent, the noise (conductance) is always increasing (constant) as a function of bias, regardless of the values of γ_L and γ_R, and the results (2) and (3) are thus recovered. A qualitatively different behavior can occur if the energy dependence is taken into account. To this purpose, it is worthwhile discussing the role of the weights γ_L and γ_R. In the present case of very large capacitive coupling, the transport properties of the wire depend in general not only on the *difference eV* between the electrochemical potentials of the two reservoirs, but on μ_L and μ_R separately, and thus on the specific values of γ_L and γ_R. This behavior is quite different from the case of weak capacitive coupling, $c/c_q \rightarrow 0$, discussed in the next section where the band bottom shift adjusts to the average value $(\mu_L + \mu_R)/2$ in order to keep the wire electroneutral. In that case, therefore, the values of γ_R and γ_L are effectively fixed,[31] whereas in the case considered here ($c \gg c_q$) they can take any value and a richer scenario arises.

For $\gamma_L \in [0,1]$, Eq. (22) yields $\partial S/\partial V \geq 0$ and the shot noise is an increasing function of bias. In contrast, for $\gamma_L > 1$, one has $\gamma_R \geq 0$ and the two terms in Eqs. (22) and (23) have competing signs. While for $V \rightarrow 0$ the positive sign prevails (as expected from the positivity of the noise and the linear conductance), the balance can be different at finite bias, depending on the energy dependence of the transmission coefficient. This is particularly interesting near a resonance, where slight variations of μ_L and μ_R can yield large variations of the product $T(E)R(E)$. In Fig. 2 we show the voltage derivative of the shot noise (solid curve) and the conductance (dotted curve) in a double-impurity wire with linear-band dispersion. Typically, the two impurities model the backscattering at nonideal contacts. The Fermi level lies near the second resonance peak shown in the inset of Fig. 2 and $\gamma_L = 3/2$. As one can see, the shot noise has a nonlinear behavior as a function of the bias and regimes of negativity in dS/dV appear. A similar behavior is exhibited by the conductance. Interestingly, when the solid curve of Fig. 2 undergoes a first dip, the dotted curve is still positive, indicating that there exist voltage ranges in which the current fluctuations decrease with bias in spite of the fact that the average current increases. This is due to the fact that, while the conductance is proportional to the transmission coefficient T, the noise depends on the combination TR, so that near a resonance the balance between the two terms in Eq. (22) can differ from the one in Eq. (23).

The voltage range in which the shot noise decreases with bias is of order $\hbar\omega_L/e$, where

$$\omega_L \doteq v_F/L, \quad (24)$$

with L being the distance between the two impurities. The energy scale $\hbar\omega_L$ corresponds to the transversal time of the
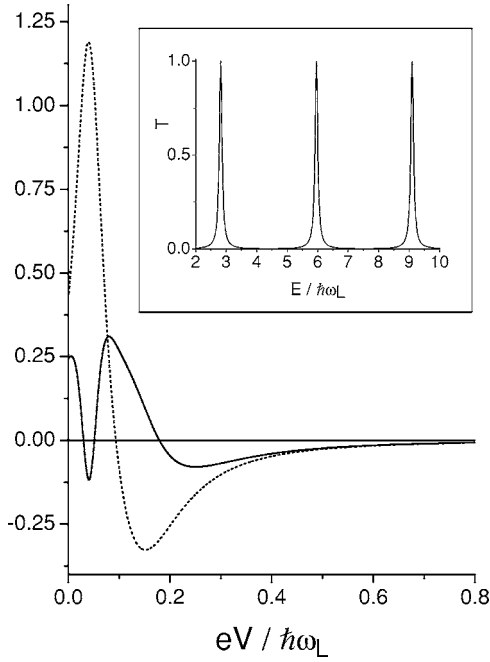
FIG. 2. The case of large capacitive coupling $c/c_q \to \infty$: Voltage derivative of the shot noise (22) in units of $e^3/2\pi\hbar$ (solid curve) and conductance (23) in units of $e^2/2\pi\hbar$ (dotted curve) as a function of bias V for a quantum wire with linear dispersion relation and two impurities of equal strength $\Lambda/\hbar v_F = 3$, located at the contacts $x_{1,2} = \pm L/2$. The electrochemical potentials are varied asymmetrically $\mu_{L/R} = E_F + \gamma_{L/R} eV$, where $\gamma_L = 3/2$ and $\gamma_R = 1/2$, and the Fermi level E_F lies near the resonance at $E_F = 5.9\hbar\omega_L$ with ω_L given by Eq. (24). At low bias $V \to 0$ the voltage derivative of the noise and the conductance are positive [due to the fact that $S(\omega=0; V=0)=0$, $S \geq 0$, and $I(V=0)=0$ with $I \geq 0$ for $V \geq 0$]. Negativity of both quantities is, however, present for a wide range of voltage values up to $eV \simeq \hbar v_F/L$, indicating that the current and the shot noise can decrease with bias. Interestingly, a decreasing noise does not necessarily correspond to a decreasing conductance. Inset: energy dependence of the transmission coefficient showing resonances.

wire of length L. For peaked resonances, like in Fig. 2, $\hbar\omega_L$ can thus be interpreted as the level spacing of the quantum dot defined by the two impurities.

While the voltage derivative of the $\omega=0$ shot noise can become negative only if $\gamma_L > 1$, at finite frequency this condition is no longer necessary.

B. Voltage dependence of finite-frequency noise

Since by now it has become experimentally relevant[6,17–20,32] to understand what happens at finite noise frequency ω, we address this regime in the following. At finite frequency, the scenario is much richer and a nonmonotonic behavior of the noise may arise even at zero temperature and even independent of the condition $\gamma_L > 1$ found for the shot noise. The generalization of Eq. (22) to finite frequencies can be readily derived and reads

$$\frac{\partial S}{\partial V}(x, \omega, V) = \frac{e^3}{2\pi\hbar} \sum_{s=\pm} s\{\theta(\omega)[\gamma_L |A_L^{LL}(\mu_L, \mu_L + s\hbar\omega; x)|^2$$

$$+ \gamma_R |A_L^{RR}(\mu_R, \mu_R + s\hbar\omega; x)|^2]$$

$$+ \theta(\hbar\omega + seV)[\gamma_L |A_L^{LR}(\mu_L, \mu_L + s\hbar\omega; x)|^2$$

$$- \gamma_R |A_L^{RL}(\mu_R, \mu_R - s\hbar\omega; x)|^2]\}, \quad (25)$$

where $\theta(x)$ is the Heaviside function and we have assumed that $E_B < \mu \pm \hbar\omega$, $\mu_R \pm \hbar\omega < E_T$. In Eq. (25), the first two and last two lines describe contributions to the voltage derivative caused by electrons originating from the same lead and from different leads, respectively. We see that Eq. (25) contains terms with competing signs. This originates from the energy dependence of the expectation values[7]

$$\langle a_{X_1 E_1}^\dagger a_{X_2 E_2} a_{X_3 E_3}^\dagger a_{X_4 E_4} \rangle - \langle a_{X_1 E_1}^\dagger a_{X_2 E_2} \rangle \langle a_{X_3 E_3}^\dagger a_{X_4 E_4} \rangle,$$

which determine the noise. Denoting by $f_{X_i}(E)$ the Fermi distribution function of the electrons incoming from lead X_i, one can easily see that at frequency ω the terms that contribute to the above expectation values come form a "Fermi box" $f_{X_1}(E)[1 - f_{X_2}(E \pm \hbar\omega)]$, the size of which depends on the applied voltage.[33] An increase of the electrochemical potential of lead X_1 (X_2) increases (decreases) the noise strength. Only if the factors $|A_L^{X_1 X_2}|^2$ are energy independent do these contributions cancel out. This occurs, for instance, in a clean quantum wire with linear band dispersion. In general, however, this is not the case. An energy dependence of these factors can arise from resonance phenomena, or from band curvature.

Let us consider the former contribution. When more than one impurity are present, Fabry-Perot resonance phenomena occur,[34,35] yielding a decrease of the noise with increasing voltage even in the absence of band curvature.[36] We shall illustrate this effect with the simplest example of a wire with linear dispersion relation and two impurities at the positions x_1 and x_2 (e.g., at the nonideal contacts). The Hamiltonian of that problem is given by $H = H_0 + H_{\mathrm{imp}}$, where H_0 is given by Eq. (14) and $H_{\mathrm{imp}} = H_{FS} + H_{BS}$, with[27,37]

$$H_{FS} = \sum_{i=1,2} \Lambda_i^{FS} (:\Psi_R^\dagger \Psi_R: + :\Psi_L^\dagger \Psi_L:)|_{x=x_i}, \quad (26)$$

$$H_{BS} = \sum_{i=1,2} \Lambda_i^{BS} (:\Psi_R^\dagger \Psi_L: + :\Psi_L^\dagger \Psi_R:)|_{x=x_i}, \quad (27)$$

where $\Psi_{R/L}(x)$ is the electron field operator for a right- or left-moving particle and x_i is the position of the ith impurity. It turns out that the forward-scattering term H_{FS} just renormalizes the Fermi velocity v_F.[27,37] In contrast, the back-scattering term H_{BS} is responsible for an energy-dependent transmission through the system.

The scattering matrix of the system can be conveniently written in terms of the elements M_{nm} of the transfer matrix $\mathsf{M}(E)$:

$$\mathsf{S}(E) = \frac{1}{M_{22}(E)}\begin{pmatrix} M_{12}(E) & 1 \\ 1 & -M_{21}^*(E) \end{pmatrix}, \quad (28)$$
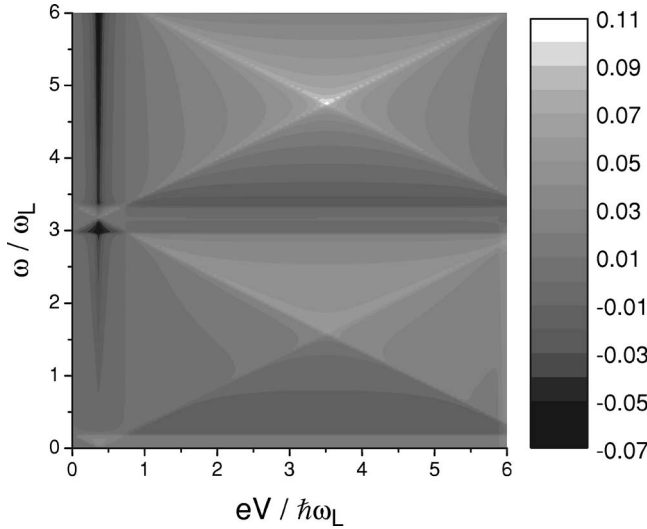
with

FIG. 3. The case of large capacitive coupling $c/c_q \to \infty$: For a quantum wire with linear dispersion relation and two impurities of equal strength $\Lambda/\hbar v_F = 10$ located at positions $x_{1,2} = \pm L/2$ the excess noise [in units of the energy $\hbar\omega_L$ associated with the ballistic frequency (24)] is shown as a function of the noise frequency ω and the applied voltage V for a measurement point at $x = -0.6L$. The values of the electrochemical potentials in the leads are $\mu_{L/R} = E_F \pm eV/2$ with $E_F = 6\hbar v_F/L$. Regions of negative excess noise are clearly visible. This negativity originates from Fabry-Perot resonance phenomena.

$$M_{12} = -i\widetilde{\Lambda}[(1 - i\widetilde{\Lambda})e^{-2ikx_1} + (1 + i\widetilde{\Lambda})e^{-2ikx_2}],$$

$$M_{22} = (1 + i\widetilde{\Lambda})^2 + \widetilde{\Lambda}^2 e^{-2ik(x_2 - x_1)}, \tag{29}$$

where $\widetilde{\Lambda} \equiv \Lambda/(\hbar v_F)$ and we have assumed (for simplicity) that $\Lambda \equiv \Lambda_1^{BS} = \Lambda_2^{BS}$. The voltage derivative of the noise can then be obtained by inserting the elements of the S matrix into Eq. (20) and the latter into Eq. (25).

We remark that while in the single-impurity case the absolute values of the entries of S do not depend on the impurity position, for two impurities these moduli depend on the phase factor $\exp(ikL)$ related to the distance $L = x_2 - x_1$ between the impurities. The transmission coefficient then exhibits resonances as a function of the energy with a typical period $\Delta E = \pi\hbar v_F/L$. In this case, even when the energy of the excitations is within the range of validity of a linearized band spectrum, the response of the system is nonlinear and quantum resonances emerge. For the average current these Fabry-Perot resonances have been observed in a recent experiment on carbon nanotubes;[35] Here, we show that these resonances also yield an oscillatory behavior of the voltage derivative of the noise and that, in particular, the excess noise (4) exhibits regions of negativity. Figure 3 displays this effect for a wire with two impurities of equal strength when the Fermi level is at resonance (corresponding to a maximum of the transmission coefficient of the system). Note that in the double-impurity setup (similar to standard quantum dot physics) the transmission depends on μ_L and μ_R and not only on their difference $eV = \mu_L - \mu_R$. The reason is that the energy

landscape of the system (i.e., the energy levels in the dot formed by the region between the two impurities) matters. Figure 3 refers to the case $\gamma_L = -\gamma_R = 1/2$; we have checked, however, that the phenomenon of negative excess noise in double-impurity systems is rather generic and not just related to a specific choice of γ_L and γ_R.

Let us now discuss the effect of band curvature. For simplicity we assume that the wire has just one impurity, in order to rule out contributions coming from resonance phenomena described above. We recall that for a wire with linear dispersion the excess noise is always non-negative.[7] In particular, $S_{EX} = 0$ for $eV < \hbar\omega$ and $S_{EX} = (e^2/2\pi\hbar)(eV - \hbar\omega)T(1 - T)$ for $eV > \hbar\omega$, with the well-known singularity at $\hbar\omega = eV$.[38] In the presence of band curvature, this result is modified, as illustrated in Fig. 4. In particular, Fig. 4(a) shows the case of a wire with parabolic dispersion

$$E_k = \frac{\hbar^2 k^2}{2m}, \tag{30}$$

whereas Fig. 4(b) depicts the case of a lattice tight-binding model (16) with dispersion

$$E_k = -4\tau \cos ka_0. \tag{31}$$

The plots depict the noise as a function of bias at a fixed value of the frequency ω. As one can see, the excess noise is negative and has a minimum around $eV \sim \hbar\omega$. For comparison, we also display by a dotted line the excess noise for a model with linear spectrum and with the same transmission coefficient at the Fermi level. The singularity at $eV = \hbar\omega$ is still evident in Fig. 4(a), whereas in Fig. 4(b) it is masked by the appearance of oscillations; in this case, the inset showing the derivative dS/dV helps to locate the singularity. The oscillations are of the type discussed in Ref. 8 and are related to the distance between the impurity and the measurement point of the noise (here chosen in the left lead, close to the contact). The fact that they appear in Fig. 4(b) and not in Fig. 4(a) is merely due to a difference in energy scales. For a lattice model energies are indeed more naturally expressed in terms of the hopping energy τ rather than the energy $\hbar\omega_L$ related to the length of the wire. In terms of a parabolic model, the case shown in Fig. 4(b) corresponds to much higher energies than in Fig. 4(a) and an oscillatory behavior becomes visible. These oscillations are due to the backscattering contributions $e^{\pm 2ik(x - x_0)}$ to the electron density (Friedel oscillations), where x_0 is the impurity position, x the measurement point, and k the electron momentum, depending on the energy through Eq. (30).

C. Experimental feasibility

As can be seen from Fig. 3, provided the bias is sufficiently high $eV \simeq \hbar\omega_L$, negative excess noise is present already at relatively low noise frequencies $\omega \lesssim 0.5\omega_L$. The effect, however, is particularly pronounced at frequencies ω of order $\pi\omega_L$ or higher. In mesoscopic devices of dimension $L \approx 1-10\ \mu$m, like quantum wires based on seminconductor heterostructures[39] or single-wall carbon nanotubes,[35,40] this corresponds to frequencies of the order of 100 GHz to a few THz (for a typical Fermi velocity v_F of order 10^6 m/s). Such
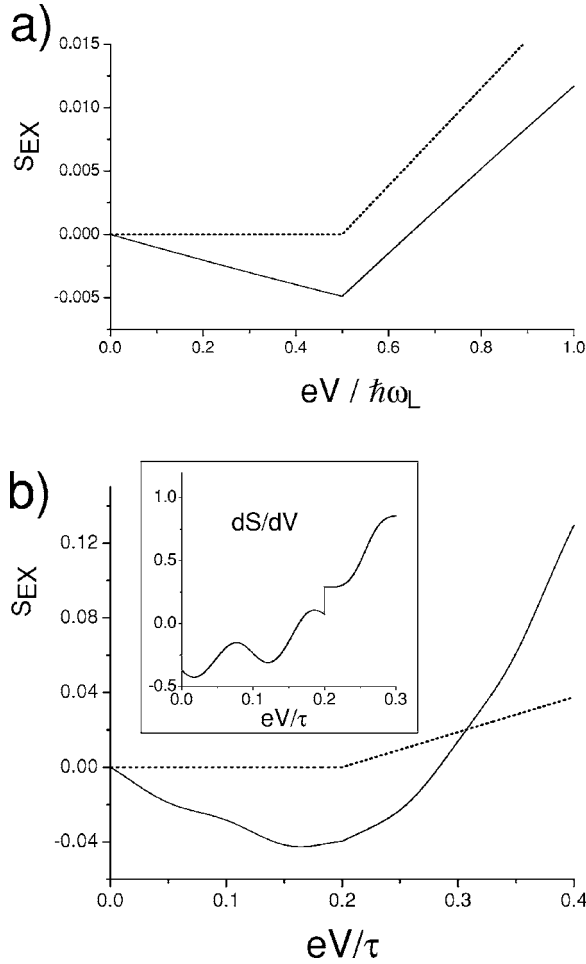
FIG. 4. The case of large capacitive coupling $c/c_q \rightarrow \infty$: negativity of the excess noise due to band curvature effects for a quantum wire with one impurity. (a) Parabolic band curvature (30). The solid curve shows the excess noise [in units of $e^2\omega_L/2\pi$ with ω_L given in Eq. (24)] as a function of the bias V for a frequency $\omega = \omega_L/2$ at the measurement point $x=-L$. The impurity of strength $\Lambda/\hbar v_F = 1$ is located in the middle; the Fermi level is $E_F = 6\hbar\omega_L$, and the bias weight is $\gamma_L = 1$. The dotted curve shows the excess noise for a wire with linear dispersion and with the same transmission coefficient at the Fermi level. (b) Sinusoidal band dispersion (31) for the tight-binding model (16). The solid curve shows the excess noise (in units of $e^2\tau/2\pi\hbar$) as a function of the bias V for a frequency $\omega = 0.2\tau/\hbar$ at the measurement point $j=-51a_0$ for a wire of length $L=100a_0$. The impurity of strength $\Lambda/a\tau = 1$ is located in the middle; the Fermi level is $E_F = \tau$, and the bias weight is $\gamma_L = 1$. The dotted curve has the same meaning as in (a). The slope dS/dV is shown as an inset.

high frequencies require a sophisticated measurement technique such as the one proposed in Ref. 5 and developed in Ref. 6. There, a detector (based on a SIS junction) and a device are capacitively coupled on chip. This allows noise detection over a large bandwidth (up to 100 GHz for Al as superconductor and up to 1 THz for Nb as superconductor). Thus, it should, in principle, be possible to observe regions of negative excess noise.

As far as the region of validity of the noninteracting theory in Sec. II B is concerned, this depends on the magni-

tude of the geometric capacitance c compared with the quantum capacitance c_q. In principle, one can create mesoscopic devices (where the conductor is, for instance, a carbon nanotube) in both the interacting or noninteracting regimes, where c_q is much larger or much smaller than c, respectively.[41] One way how the ratio c/c_q can be controlled is by changing the dielectric constant of the substrate, which changes only c and not c_q. Apart from the dielectric constant of the medium, c depends on the shape and dimensions of the sample as well as on its distance to the conducting plane.

III. CASE OF FINITE CAPACITANCE

We now discuss the effects of a finite capacitive coupling (11) between a wire of length L and the gate. As mentioned in the Introduction, a finite capacitance induces a finite (frequency-dependent) band-bottom shift in the wire, which in turn affects the current in the wire, yielding essentially an interacting transport problem. One way to face this problem is to generalize the scattering matrix formalism: the scattering matrix S depends in fact not only on the electron energy E, but also on the potential profile U, so that the coefficients $A^{X_1X_2}$ in Eq. (20) have to be modified accordingly $A^{X_1X_2} \rightarrow A^{X_1X_2} + \Delta A^{X_1X_2}$. This approach has been introduced by Büttiker and co-workers in a series of seminal papers[42–46] and was recently applied to the description of quantum point contacts and chaotic cavities.[47,48] An alternative way is to determine self-consistently the electron density taking into account both the bare charge injected by the leads and the charge induced by the fluctuations of the potential U through the polarization propagator $\Pi(x,x')$. This technique has been successfully applied[49,24] to the case of a clean multichannel quantum wire. In presence of impurities, however, this method is practicable only for weak potential U and is therefore not suitable to investigate the regime of small capacitance.

Here we shall thus adopt another approach which allows us to explore the full range of c/c_q and to account for impurities as well. We shall exploit a mapping to a Luttinger liquid. It is, in fact, well known[24,25,50,51] that in the case that band curvature effects can be neglected, the problem of a quantum wire with a geometric capacitance c with respect to a gate can be mapped onto a Luttinger liquid with interaction strength

$$g = \frac{1}{\sqrt{1 + \dfrac{c_q}{c}}}, \tag{32}$$

where $c_q = e^2/\pi\hbar v_F$ is the quantum capacitance. The case of large geometrical capacitance $c \gg c_q$ treated in the previous section corresponds to $g=1$ (no charge screening), whereas the opposite limit of $c \ll c_q$—i.e., $g \rightarrow 0$—corresponds to a completely electroneutral wire (full charge screening). In any intermediate case, only a fraction $1-g^2$ of the charge is screened.[51] Notice also that the parameter g is strictly related to the electrochemical capacitance[43] per unit length

$$\frac{1}{c_\mu} = \frac{1}{c} + \frac{1}{c_q} \qquad (33)$$

and to the charge-relaxation time[47]

$$t_\mu = \frac{h}{e^2} c_\mu L \qquad (34)$$

through the relation

$$c_\mu = g^2 \frac{e^2}{\pi \hbar v_F}. \qquad (35)$$

The charge-relaxation time is therefore determined by the timescale of the wire uncoupled to the gate (typically the ballistic time L/v_F) in the limit of $c/c_q \gg 1$ and by the RC time $t_{RC} = (h/e^2)cL$ in the limit of $c/c_q \ll 1$. This is in accordance with the results of a recent investigation[48] of the noise in mesoscopic chaotic cavities coupled to a gate. Typically, it is the charge-relaxation time that determines the dynamical time scales of transport in a mesoscopic conductors.[52]

The mapping to the Luttinger liquid model is realized through the standard bosonized representation[53] of electron field operators

$$\Psi_{R/L}(x) = \frac{\eta_{R/L}}{\sqrt{2\pi a}} e^{\pm i\sqrt{4\pi}\Phi_{R/L}(x)}, \qquad (36)$$

where a is the cutoff length, $\eta_{R/L}$ are Majorana fermions (Klein factors), and $\Phi_{R/L}$ are nonlocal plasmonic excitation fields. Introducing the usual Bose field operator $\Phi = \Phi_R + \Phi_L$ and its conjugate momentum $\Pi = \partial_x(\Phi_R - \Phi_L)$, the Hamiltonian reads $H = H_{LL} + H_{imp}$ with

$$H_{LL} = \frac{\hbar v_F}{2} \int_{-\infty}^{\infty} dx \left[\Pi^2 + \frac{1}{g^2(x)}(\partial_x \Phi)^2 \right], \qquad (37)$$

$$H_{imp} = \sum_i \lambda_i \cos[\sqrt{4\pi}\Phi(x_i) + 2k_F x_i]. \qquad (38)$$

The first term H_{LL} describes the band kinetics of the quantum wire (14) as well as its capacitive coupling (11) to the gate. Note that the Luttinger liquid parameter (32) in the Hamiltonian (37) is inhomogeneous. Indeed, although the capacitive coupling is finite $(0 < g < 1)$ over the length L of the wire (see Fig. 1), we have an effectively large geometrical capacitance $(g = 1)$ in the regions of the leads. This is because, as far as transport properties of the wire are concerned, the leads can be modeled as ideal Fermi gases with electrochemical potentials μ_R and μ_L which determine the energy of the electrons *injected* into the gated wire. A step-like approximation for $g(x)$ is valid when the change of the capacitive coupling at the ends of the wire occurs over a distance much larger than the Fermi wavelength and much smaller than the length of the wire. The second term (38) of H represents the backscattering by impurities at positions x_i, which introduces a strong nonlinearity in the field Φ. The bosonized expression for the current electron operator reads[53]

$$j(x) = \frac{e v_F}{\sqrt{\pi}} \Pi(x), \qquad (39)$$

and the noise can be computed by inserting Eq. (39) into Eq. (1), yielding

$$S(x,\omega,V) = S_0(x,\omega) + S_{imp}(x,\omega,V). \qquad (40)$$

In the above equation, the first term describes the noise in the absence of impurities, which can be computed exactly since the Hamiltonian (37) is quadratic. The second term accounts for the effect of the impurities (38), which can be treated perturbatively within the nonequilibrium Keldysh formalism.[54]

We recall that, in the absence of impurities, due to the linear spectrum of the Hamiltonian, the noise S_0 does not depend on the voltage,[55] and therefore the excess noise for a clean wire is vanishing. On the other hand, in the presence of more than one impurity, Fabry-Perot resonance phenomena arise, which for $c/c_q \to \infty$ were shown in Sec. II to lead to negative excess noise. Not surprisingly, this behavior survives also for finite capacitive coupling, as recent results for Luttinger liquids at high frequencies show [see Figs. 7(c) and 9(a) of Ref. 36].

The case of a single impurity in an adiabatically contacted wire is therefore peculiar since Fabry-Perot interferences are absent. This is the simplest example in which a finite capacitance can yield notable and clearly identifiable differences with respect to the case of large capacitive coupling, and we shall thus focus on this situation.

A. Voltage dependence of zero-frequency noise

In a one-dimensional (1D) wire with one impurity a capacitive coupling (11) to a gate has dramatic effects on the transport properties. The interplay of Friedel oscillations with density-density correlations leads to a strong renormalization of the impurity strength by the coupling to the gate, driving the wire at $T = 0$ into an insulating state.[56] Electron transport only occurs at finite bias and, in particular, for $eV \gg \lambda^*$, where $\lambda^* = \hbar\omega_c(\lambda/\hbar\omega_c)^{1/(1-g)}$ is the renormalized impurity strength[27,56,57] at bandwidth $\hbar\omega_c$. A similar behavior occurs in a one-channel coherent conductor in series with an Ohmic environment.[58]

Thus, in the presence of a capacitive coupling, the voltage dependence of the noise is not trivial: even at zero frequency (shot noise), it can significantly deviate from the result (2) obtained for $c/c_q \to \infty$. The method how to calculate noise properties within the bosonization formalism has been expounded in Ref. 57. Here we use these earlier results to elucidate the effects of finite capacitive coupling. The shot noise of a gated quantum wire in the weak backscattering limit is proportional to the backscattering current[59]

$$S(\omega = 0, V) = e I_{BS}(V). \qquad (41)$$

Here I_{BS} is the part of the transmitted current I that is backscattered by the impurities—explicitly,

$$I = \frac{e^2}{2\pi\hbar} V - I_{\mathrm{BS}}, \qquad (42)$$

where the first term represents the current for the wire without impurities. Equation (41) has the same form as the relation between shot noise and backscattering current obtained for infinite capacitive coupling $c/c_q \to \infty$ in the presence of a weak impurity. In that case, indeed, the shot noise is just given by Eq. (2) for the case of a single channel with $T \simeq 1$, whereas $I_{\mathrm{BS}} = (e^2/2\pi\hbar)V(1-T)$, as easily obtained from Eqs. (3) and (42). Here, however, the finite capacitive coupling entails a dependence of I_{BS} on the bias voltage V that differs significantly from a mere proportionality, the latter being only valid in the regime $c/c_q \to \infty$. Now, one rather obtains[60]

$$I_{\mathrm{BS}}(V) = I_{\mathrm{BS}}^{\infty}(V)[1 + f_{\mathrm{BS}}(eV/\hbar\omega_L)]. \qquad (43)$$

In Eq. (43), the first factor shows power law behavior as a function of the bias,[56]

$$I_{\mathrm{BS}}^{\infty}(V) = \frac{e^2}{2\pi\hbar} V \frac{\pi^2}{\Gamma(2g)} \left(\frac{\lambda^*}{eV} \right)^{2(1-g)}, \qquad (44)$$

and the corresponding exponent is directly related to the capacitive coupling through the parameter (32). The second factor describes oscillatory deviations from $I_{\mathrm{BS}}^{\infty}(V)$ related to the finite length of the wire through the ballistic frequency (24). Details about the explicit form of f_{BS} can be found in Ref. 57. Here we just mention that f_{BS} decays for $eV \gg \hbar\omega_L$. The general trend of the shot noise as a function of the applied bias is thus determined by $I_{\mathrm{BS}}^{\infty}(V)$, and one obtains

$$\frac{\partial S}{\partial V}(\omega = 0, V) \simeq (2g-1) \frac{e^3}{\hbar} \frac{\pi}{\Gamma(2g)} \left(\frac{\lambda^*}{eV} \right)^{2(1-g)}. \qquad (45)$$

For $1/2 < g < 1$—i.e., for $c > c_q/3$—the voltage derivative is positive and, in particular, in the limit $g \to 1$, the result (2) for large capacitance (in the special case of weak impurity backscattering) is recovered. In contrast, for

$$c < \frac{c_q}{3}, \qquad (46)$$

the shot noise *decreases* with increasing voltage.

B. Voltage dependence of finite-frequency noise

At finite frequency, the differences with respect to the case $c \gg c_q$ are even more striking. We recall that in the latter regime the excess noise of a quantum wire with linear dispersion and one (weak) impurity is $S_{\mathrm{EX}} = 0$ for $eV < \hbar\omega$ and $S_{\mathrm{EX}} = (e^2/2\pi\hbar)(eV - \hbar\omega)R$ for $eV > \hbar\omega$, R being the reflection coefficient. While there are no Fabry-Perot resonances for a single impurity, when c/c_q is finite, another type of resonance phenomena occurs due to the difference in capacitive coupling strength between the gated region and the metallic lead region. Indeed, when an interacting 1D wire is connected to metallic leads backscattering can occur at adiabatic contacts due to Andreev-like reflections of plasmonic charge excitations.[61] Finite-length effects thus emerge.

Using Eq. (40) and recalling the fact that the term S_0 does not depend on the bias voltage V, the excess noise can be written as
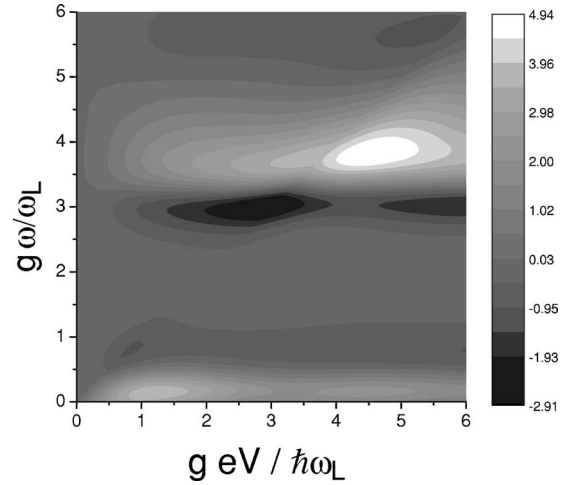

FIG. 5. Excess noise for a gated wire with capacitance $c = c_q/10$, with an impurity shifted by $L/4$ off the center of the wire. The measurement point is at $x = -0.6L$. Regions of negative excess noise are visible at frequencies $\omega \sim \pi\omega_L/g$, where ω_L is the ballistic frequency (24) and g is the parameter defined in Eq. (32).

$$S_{\mathrm{EX}}(x, \omega, V) = S_{\mathrm{imp}}(x, \omega, V) - S_{\mathrm{imp}}(x, \omega, V = 0). \qquad (47)$$

Here the term $S_{\mathrm{imp}}(x, \omega, V)$ can be shown to be a product of a local current correlator, which depends on the voltage V, evaluated at the impurity position x_0 and the clean-wire nonlocal retarded correlator between the measurement point x and the impurity position x_0 (see Ref. 57 for details). The Andreev-type reflections enter directly in these correlators, so that the interference phenomena between Andreev-type reflected plasmonic charge excitations and modes backscattered at the impurity give rise to notable structure in the voltage-frequency diagram of the excess noise, as illustrated in Fig. 5 for the case of a small capacitance $c = c_q/10$. Regions of negative excess noise are present at frequencies of order ω_L/g. In Fig. 5 the noise is taken in its symmetrized version and the impurity is off centered at $x_0 = L/4$; results for the more special case of a centered impurity can be found in Ref. 57.

IV. CONCLUSIONS

We have shown that in the quantum regime the current noise of a quantum wire capacitively coupled to a gate can decrease with increasing applied voltage. Both the shot noise and the finite-frequency noise have been analyzed in different regimes, ranging from large to small ratios c/c_q, where c is the geometrical and $c_q = e^2\nu$ the quantum capacitance. In particular, in the regime of large capacitive coupling $c \gg c_q$, the noise can decrease with increasing bias voltage when the transmission coefficients are energy dependent. This can occur either in the presence of Fabry-Perot resonances, like, for instance, in a nonideally contacted wire, or because of band curvature effects. In both cases we have shown that excess noise can be negative.

When the coupling to the gate is of order c_q, even for an energy-independent transmission coefficient, and in the absence of Fabry-Perot resonances or band curvature, the noise

exhibits rich structure which can significantly deviate from the usual expression (2). For instance, for an adiabatically contacted wire with one impurity, when the geometrical capacitance is smaller than $c_q/3$, the shot noise decreases with bias as a power law. At finite frequency, Andreev-type resonances due to the finite length of the wire induce negativity of the excess noise. We have thus demonstrated that the quantity usually termed *excess* noise can become negative even at zero temperature. Furthermore, we have estimated that such negative excess noise can be observed with state-of-the-art techniques using on-chip noise detection

schemes.[5,6] We therefore expect that these predictions can be verified in current experimental realizations of ballistic 1D conductors, such as quantum wires based on GaAs/AlGaAs heterostructures[39] or single-wall carbon nanotubes.[35,40]

[1] H. B. Callen and T. A. Welton, Phys. Rev. **83**, 34 (1951).

[2] G. B. Lesovik and R. Loosen, JETP Lett. **65**, 295 (1997).

[3] L. D. Landau and E. M. Lifshitz, *Statistical Physics*, 3rd ed. (Butterworths Heinemann, London, 1997), pt. 1.

[4] S. Kogan, *Electronic Noise and Fluctuations in Solids* (Cambridge University Press, Cambridge, England, 1996).

[5] R. Aguado and L. P. Kouwenhoven, Phys. Rev. Lett. **84**, 1986 (2000).

[6] R. Deblock, E. Onac, L. Gurevich, and L. P. Kouwenhoven, Science **301**, 203 (2003).

[7] Y. M. Blanter and M. Büttiker, Phys. Rep. **336**, 1 (2000).

[8] B. Trauzettel and H. Grabert, Phys. Rev. B **67**, 245101 (2003).

[9] V. A. Khlus, Sov. Phys. JETP **66**, 1243 (1987).

[10] G. B. Lesovik, JETP Lett. **49**, 592 (1989).

[11] M. Büttiker, Phys. Rev. Lett. **65**, 2901 (1990).

[12] B. Trauzettel, I. Safi, F. Dolcini, and H. Grabert, Phys. Rev. Lett. **92**, 226405 (2004).

[13] H.-A. Engel and D. Loss, Phys. Rev. Lett. **93**, 136602 (2004).

[14] A. V. Lebedev, A. Crépieux, and T. Martin, Phys. Rev. B **71**, 075416 (2005).

[15] K.-V. Pham, cond-mat/0504389 (unpublished).

[16] D. Bagrets and F. Pistolesi, cond-mat/0606775 (unpublished).

[17] R. J. Schoelkopf, P. J. Burke, A. A. Kozhevnikov, D. E. Prober, and M. J. Rooks, Phys. Rev. Lett. **78**, 3370 (1997).

[18] E. Onac, F. Balestro, B. Trauzettel, C. F. J. Lodewijk, and L. P. Kouwenhoven, Phys. Rev. Lett. **96**, 026803 (2006).

[19] P.-M. Billangeon, F. Pierre, H. Bouchiat, and R. Deblock, Phys. Rev. Lett. **96**, 136804 (2006).

[20] E. Onac, F. Balestro, L. H. Willems van Beveren, U. Hartmann, Y. V. Nazarov, and L. P. Kouwenhoven, Phys. Rev. Lett. **96**, 176601 (2006).

[21] G. B. Lesovik and R. Loosen, Z. Phys. B: Condens. Matter **91**, 531 (1993).

[22] O. M. Bulashenko and J. M. Rubì, Physica E (Amsterdam) **17**, 638 (2003).

[23] N. Wiener, Acta Math. **55**, 117 (1930); A. Khintchine, Math. Ann. **109**, 604 (1934).

[24] Ya. M. Blanter, F. W. J. Hekking, and M. Büttiker, Phys. Rev. Lett. **81**, 1925 (1998).

[25] I. Safi, Eur. Phys. J. B **12**, 451 (1999).

[26] The coupling to the gate has negligible effects on the metallic leads, due to their electroneutrality, and is therefore assumed to be zero here.

[27] J. von Delft and H Schöller, Ann. Phys. **4**, 225 (1998).

[28] Regarding the appropriate current operator we refer to Eq. (13) for a parabolic dispersion band, to Eq. (15) for a Dirac linearized band, and to Eq. (17) for a lattice tight-binding model.

[29] Similar equations for the coefficients (20) have been obtained in Ref. 7; there, however, the assumptions of a linearized band and energy independent transmission were immediately made in order to simplify the treatment.

[30] L. P. Kouwenhoven (private communication).

[31] For an energy-independent transmission coefficient, for instance, one effectively has $\mu_{L/R}=E_F\pm eV/2$. In other situations, the determination of the band-bottom shift is more involved. For resonant tunneling see, e.g., Ref. 42.

[32] L.-H. Reydellet, P. Roche, D. C. Glattli, B. Etienne, and Y. Jin, Phys. Rev. Lett. **90**, 176803 (2003).

[33] The expression "Fermi box" seems to be evocative here, since the expression $f_{X_1}(E)[1-f_{X_2}(E\pm\hbar\omega)]$ as a function of energy E has the shape of a box. At zero temperature it is indeed 1 for $\mu_{X_1} \leq E \leq \mu_{X_2} \mp \hbar\omega$ and 0 elsewhere.

[34] C. S. Peca, L. Balents, and K. J. Wiese, Phys. Rev. B **68**, 205423 (2003).

[35] W. Liang, M. Bockrath, D. Bozovic, J. H. Hafner, M. Tinkham, and H. Park, Nature (London) **411**, 665 (2001).

[36] P. Recher, N. Y. Kim, and Y. Yamamoto, cond-mat/0604613 (unpublished).

[37] See Sec. 3.3 of H. Grabert, in *Exotic States in Quantum Nanostructures*, edited by S. Sarkar (Kluwer, Dordrecht, 2002); cond-mat/0107175.

[38] G. B. Lesovik, JETP Lett. **70**, 208 (1999).

[39] R. de Picciotto, H. L. Stormer, L. N. Pfeiffer, K. W. Baldwin, and K. W. West, Nature (London) **411**, 51 (2001); A. Yacoby, H. L. Stormer, N. S. Wingreen, L. N. Pfeiffer, K. W. Baldwin, and K. W. West, Phys. Rev. Lett. **77**, 4612 (1996); A. Yacoby, H. L. Stormer, N. S. Wingreen, L. N. Pfeiffer, K. W. Baldwin, and K. W. West, Solid State Commun. **101**, 77 (1997); S. Tarucha, T. Honda, and T. Saku, *ibid.* **94**, 413 (1995).

[40] M. Bockrath, D. H. Cobden, J. Lu, A. G. Rinzler, R. E. Smalley, L. Balents, and P. L. McEuen, Nature (London) **397**, 598 (1999); C. T. White and T. N. Todorov, *ibid.* **393**, 240 (1998); C. Dekker, Phys. Today **52**, 22 (1999); S. Tans, M. H. Devoret, H. Dai, A. Thess, R. E. Smalley, L. J. Geerligs, and C. Dekker, Nature (London) **386**, 474 (1997).

[41] S. Ilani, L. A. K. Donev, M. Kindermann, and P. L. McEuen, Nat. Phys. **2**, 687 (2006); S. Ilani (private communication).

[42] T. Christen and M. Büttiker, Europhys. Lett. **35**, 523 (1996).

[43] M. Büttiker, H. Thomas, and A. Prêtre, Phys. Lett. A **180**, 364 (1993).

[44] M. Büttiker, A. Prêtre, and H. Thomas, Phys. Rev. Lett. **70**, 4114 (1993); M. Büttiker, J. Phys.: Condens. Matter **5**, 9361 (1993).

[45] P. W. Brouwer and M. Büttiker, Europhys. Lett. **37**, 441 (1997).

[46] K. E. Nagaev, S. Pilgram, and M. Büttiker, Phys. Rev. Lett. **92**, 176804 (2004).

[47] M. H. Pedersen, S. A. van Langen, and M. Büttiker, Phys. Rev. B **57**, 1838 (1998).

[48] F. W. J. Hekking and J. P. Pekola, Phys. Rev. Lett. **96**, 056603 (2006).

[49] Ya. M. Blanter and M. Büttiker, Europhys. Lett. **42**, 535 (1998).

[50] L. I. Glazman, I. M. Ruzin, and B. I. Shklovskii, Phys. Rev. B **45**, 8454 (1992).

[51] R. Egger and H. Grabert, Phys. Rev. Lett. **79**, 3463 (1997).

[52] For chaotic cavities in the regime $c \ll c_q$ there exist exceptions to this general statement. In situations where weak localization effects become relevant, for instance, the ac conductance fluctuations are governed by the dwell time (see Ref. 45). Similarly, the latter also enters in the third cumulant of the electrical current (see Ref. 46).

[53] A. O. Gogolin, A. A. Nersesyan, and A. M. Tsvelik, *Bosonization and Strongly Correlated Systems* (Cambridge University Press, Cambridge, England, 1998); T. Giamarchi, *Quantum Physics in One Dimension* (Oxford University Press, Oxford, 2004).

[54] L. V. Keldysh, Zh. Eksp. Teor. Fiz. **47**, 1515 (1964) L. V. Keldysh, [Sov. Phys. JETP **20**, 1018 (1965)]; H. Kleinert, *Path Integrals in Quantum Mechanics, Statistics, and Polymer Physics* (World Scientific, Singapore, 1995).

[55] C. de C. Chamon, D. E. Freed, and X. G. Wen, Phys. Rev. B **53**, 4033 (1996).

[56] C. L. Kane and M. P. A. Fisher, Phys. Rev. B **46**, 15233 (1992).

[57] F. Dolcini, B. Trauzettel, I. Safi, and H. Grabert, Phys. Rev. B **71**, 165309 (2005).

[58] I. Safi and H. Saleur, Phys. Rev. Lett. **93**, 126602 (2004).

[59] C. L. Kane and M. P. A. Fisher, Phys. Rev. Lett. **72**, 724 (1994); V. V. Ponomarenko and N. Nagaosa, Phys. Rev. B **60**, 16865 (1999); B. Trauzettel, R. Egger, and H. Grabert, Phys. Rev. Lett. **88**, 116401 (2002).

[60] F. Dolcini, H. Grabert, I. Safi, and B. Trauzettel, Phys. Rev. Lett. **91**, 266402 (2003).

[61] I. Safi and H. J. Schulz, Phys. Rev. B **52**, R17040 (1995).